[redacted]

CENTRAL RESEARCH LIBRARY
DOCUMENT COLLECTION

4

AEC RESEARCH AND DEVELOPMENT REPORT

ORNL-2187
C-84 – Reactors-Special
Features of Aircraft Reactors

DECLASSIFIED
CLASSIFICATION CHANGED TO: AEC 11-24-59
BY AUTHORITY OF: [illegible]
BY: [illegible]

MARTIN MARIETTA ENERGY SYSTEMS LIBRARIES
3 4456 0350341 1

FORCED CONVECTION IN THE HELICAL PIPE OF THE ANP IN-PILE LOOP

N. D. Greene
L. D. Palmer
H. F. Poppendiek
G. M. Winn

CENTRAL RESEARCH LIBRARY
DOCUMENT COLLECTION
LIBRARY LOAN COPY
DO NOT TRANSFER TO ANOTHER PERSON
If you wish someone else to see this document, send in name with document and the library will arrange a loan.

OAK RIDGE NATIONAL LABORATORY
OPERATED BY
UNION CARBIDE NUCLEAR COMPANY
A Division of Union Carbide and Carbon Corporation
UCC
POST OFFICE BOX P · OAK RIDGE, TENNESSEE

[redacted]

LEGAL NOTICE

This report was prepared as an account of Government sponsored work. Neither the United States, nor the Commission, nor any person acting on behalf of the Commission:

A. Makes any warranty or representation, express or implied, with respect to the accuracy, completeness, or usefulness of the information contained in this report, or that the use of any information, apparatus, method, or process disclosed in this report may not infringe privately owned rights; or

B. Assumes any liabilities with respect to the use of, or for damages resulting from the use of any information, apparatus, method, or process disclosed in this report.

As used in the above, "person acting on behalf of the Commission" includes any employee or contractor of the Commission to the extent that such employee or contractor prepares, handles or distributes, or provides access to, any information pursuant to his employment or contract with the Commission.

[redacted]

[redacted]

Contract No. W-7405, eng 26

Reactor Experimental Engineering Division

FORCED CONVECTION IN THE HELICAL PIPE OF THE ANP IN-PILE LOOP

by

N. D. Greene
L. D. Palmer
H. F. Poppendiek
G. M. Winn

DATE ISSUED:

NOV 8 1956

OAK RIDGE NATIONAL LABORATORY
Operated by
UNION CARBIDE NUCLEAR COMPANY
A Division of Union Carbide and Carbon Corporation
Post Office Box P
Oak Ridge, Tennessee

[redacted]

MARTIN MARIETTA ENERGY SYSTEMS LIBRARIES
3 4456 0350341 1

[redacted]

ORNL-2187
C-84 - Reactors-Special
Features of Aircraft Reactors
M-3679 (18th ed.)

INTERNAL DISTRIBUTION

1. C. E. Center
2. Biology Library
3. Health Physics Library
4-5. Central Research Library
6. Reactor Experimental Engineering Library
7-13. Laboratory Records Department
14. Laboratory Records, ORNL R.C.
15. A. M. Weinberg
16. L. B. Emlet (K-25)
17. J. P. Murray (Y-12)
18. J. A. Swartout
19. E. H. Taylor
20. E. D. Shipley
21. C. E. Winters
22. M. L. Nelson
23. W. H. Jordan
24. R. R. Dickison
25. S. C. Lind
26. F. L. Culler
27. A. H. Snell
28. A. Hollaender
29. M. T. Kelley
30. J. A. Lane
31. K. Z. Morgan
32. T. A. Lincoln
33. A. S. Householder
34. C. S. Harrill
35. D. S. Billington
36. D. W. Cardwell
37. E. M. King
38. L. G. Alexander
39. S. E. Beall
40. E. S. Bettis
41. E. P. Blizard
42. E. G. Bohlmann
43. W. F. Boudreau
44. G. E. Boyd
45. R. B. Briggs
46. H. C. Claiborne
47. S. I. Cohen
48. J. A. Conlin
49. C. M. Copenhaver
50. G. A. Cristy
51. S. J. Cromer
52. C. W. Cunningham
53. J. H. Devan
54. D. A. Douglas
55. E. R. Dytko
56. W. K. Ergen
57. A. P. Fraas
58. R. I. Gray
59. N. D. Greene
60. D. P. Gregory
61. W. R. Grimes
62. H. W. Hoffman
63. G. W. Keilholtz
64. A. S. Kitzes
65. C. G. Lawson
66. F. E. Lynch
67. R. N. Lyon
68. W. D. Manly
69. G. L. Muller
70. L. D. Palmer
71. A. M. Perry
72. H. F. Poppendiek
73. W. D. Powers
74. H. W. Savage
75. R. D. Schultheiss
76. O. Sisman
77. M. J. Skinner
78. P. E. Stover
79. D. G. Thomas
80. D. B. Trauger
81. J. E. Wantland
82. G. D. Whitman
83. M. M. Yarosh
84. ORNL - Y-12 Technical Library, Document Reference Section

EXTERNAL DISTRIBUTION

85. Division of Research and Development, AEC, ORO
86-197. Given distribution as shown in M-3679 under Reactors-Special Features of Aircraft Reactors category

TABLE OF CONTENTS

	Page
SUMMARY	1
NOMENCLATURE	2
INTRODUCTION	4
EXPERIMENTAL STUDIES	7
COMPARISON OF EXPERIMENTAL AND PREDICATED TEMPERATURE DISTRIBUTIONS	14
CONCLUDING REMARKS	16
APPENDIX	17

[redacted]

SUMMARY

This report concerns itself with a study of the temperature structure within a circulating-fuel that is flowing through a helical pipe in the ANP In-pile Loop. This helix is exposed to the neutron flux field of the MTR. An experimental study of the temperature distribution within a fluid flowing through a glass model of the ANP In-pile Loop is presented; the volumetric heat sources within the fluid are generated electrically. An approximate mathematical analysis of the temperature structure in the helix system is outlined and the resulting calculations are compared with experimental results obtained in the volume-heat-source system. This study indicates that large wall temperature differences can exist around the periphery of the helix because of the asymmetry in the hydrodynamic structure. The resulting wall-temperature asymmetry is an important parameter that must be taken into account when analyzing the mass transfer and corrosion processes in the ANP In-pile Loop.

[redacted]

[redacted]

NOMENCLATURE

Letters

A	heat transfer cross sectional area, ft^2
A_e	electrical current cross sectional area, ft^2
a	fluid thermal diffusivity, ft^2/hr
c_p	fluid heat capacity, Btu/lb ^oF
D	pipe diameter, ft
E	electrical potential, volts
k	fluid thermal conductivity, Btu/hr ft^2 ($^oF/ft$)
L	axial distance along helix, ft
P	electrical heat source, watts
q	heat transfer rate, Btu/hr
r	radial distance, ft
r_d	radial position at which the reference temperature t_d is stipulated, ft
r_h	radial distance from helix center, ft
r_i	inner sector radius, ft
r_o	outer sector radius, ft
R_e	electrical resistance, ohms
t	fluid temperature, ^oF
$t_{\mathbb{C}}$	fluid centerline temperature, ^oF
t_d	temperature datum, ^oF
t_i	inner wall temperature, ^oF
$t_{m_{in}}$	mixed-mean fluid inlet temperature, ^oF
$t_{m_{out}}$	mixed-mean fluid outlet temperature, ^oF

[redacted]

t_o	outer wall temperature, ^oF
u	axial fluid velocity distribution, ft/hr
u_{max}	maximum fluid velocity, ft/hr
$\bar{u}$	mean fluid velocity in helix, ft/hr
$\bar{u}_i$	mean fluid velocity of inner sector, ft/hr
$\bar{u}_o$	mean fluid velocity of outer sector, ft/hr
$\bar{u}_s$	mean fluid velocity of sector, ft/hr
V	fluid volume, ft^3
W	volume heat source distribution, Btu/hr ft^3
$\bar{W}$	mean volume heat source, Btu/hr ft^3
y	radial distance from inner wall, ft
γ	fluid weight density, lbs/ft^3
ϵ	eddy diffusivity, ft^2/hr
ν	kinematic viscosity, ft^2/hr
ρ_e	electrical resisivity, ohm-ft
ϕ	angle subtended by helical radii, r_h

Dimensionless Moduli

$$n = \frac{y}{r_i}$$

$$Pr = \frac{\nu \gamma c_p}{k}, \quad \text{Prandtl Modulus}$$

$$Re = \frac{\bar{u}D}{\nu}, \quad \text{Reynolds Modulus for helix}$$

$$Re_i = \frac{\bar{u}_i 2r_i}{\nu}, \quad \text{Reynolds Modulus for inner sector}$$

$$Re_o = \frac{\bar{u}_o 2r_o}{\nu}, \quad \text{Reynolds Modulus for outer sector}$$

INTRODUCTION

Upon examining the wall corrosion in pipe bends of out-of-pile corrosion loops, the metallurgists discovered that the corrosion rate was not uniform. It was observed that on the short radius or inner side the corrosion rate was consistently several times as great as that on the long radius or outer side. It was suggested that this difference in corrosion was related to the fact that the wall temperatures were likewise not uniform in the pipe bend, thus perhaps creating a corrosion or mass transfer potential difference. For this reason the task of obtaining information on the hydrodynamic and thermal structures within the fluids circulating through pipe bends was initiated.

The ANP Project has used a helix (see Figure 1) which is part of an In-pile Loop located in a high neutron flux field in the MTR thereby yielding high volume-heat-sources both in the pipe wall and the fuel. Before the first In-pile Loop was put into the MTR, approximate calculations were made on the temperature asymmetry in the helix (reference 1). At present, operational and thermocouple difficulties have made it impossible to obtain much experimental information on the temperature structure in the helix under actual operating conditions in the MTR. However, the data which were obtained appeared to be in general agreement with the previous approximate calculations.

Because of the difficulties and uncertainties that appeared to be associated with obtaining experimental temperature information from the In-pile Loop, a simpler and more accurate experimental system was devised. In the following

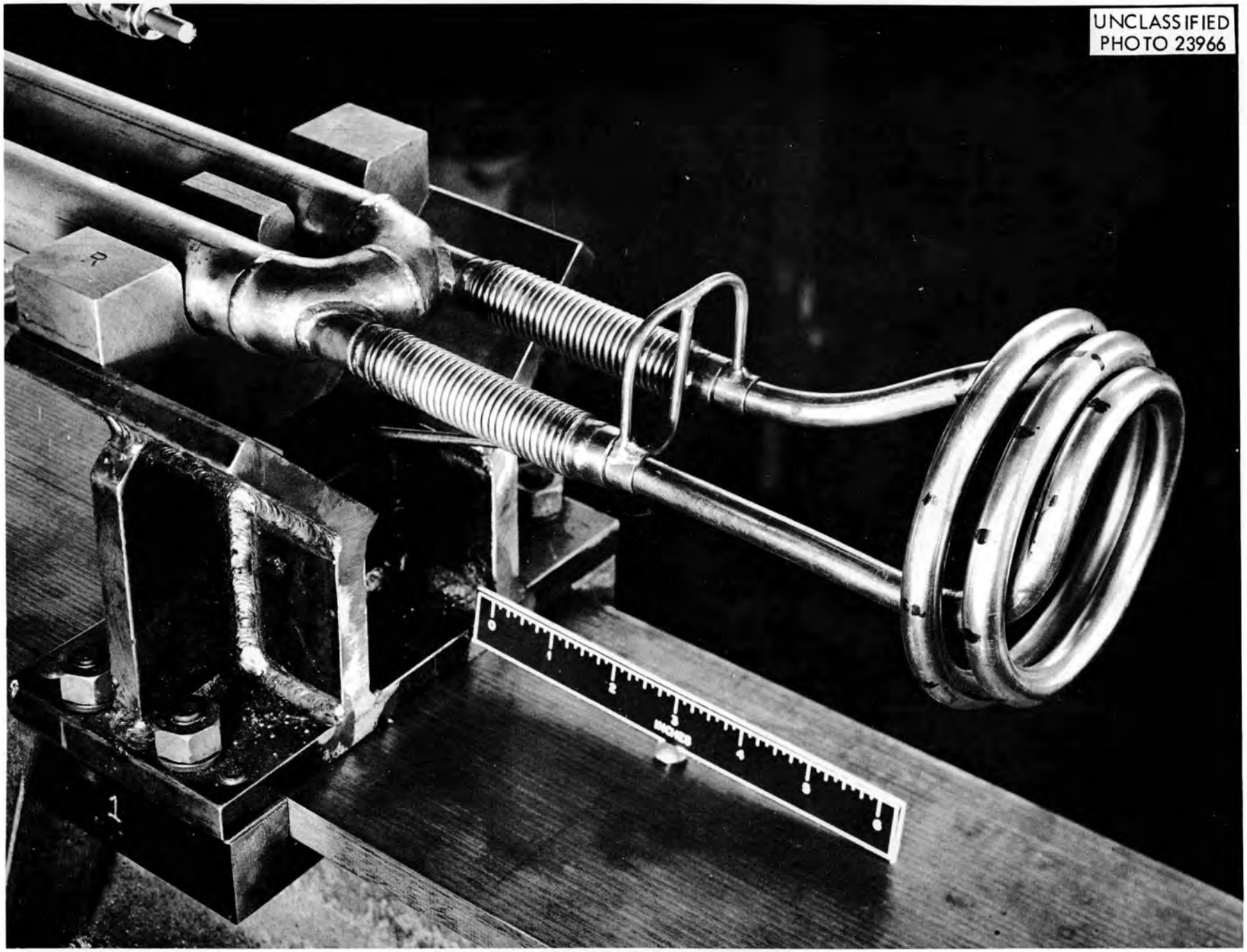

Fig. 1. ANP "In-Pile Loop Helix". ([redacted] with title)

paragraphs, experimental temperature distributions in a glass model of the ANP helix are presented. The volume heat sources were generated electrically within electrolytes which were circulated through the system; no volume heat sources existed in the glass walls. An approximate mathematical analysis of the temperature structure in the helix is outlined, and the results are compared to experimental measurements.

EXPERIMENTAL STUDIES

Hydrodynamics

Prior to the heat transfer experiments which are described below, a study of the velocity structure in the helix of the In-pile Loop was conducted. A literature survey yielded useful although incomplete quantitative information on the hydrodynamic structure in pipe bends. Also, the velocity distributions within the helix were visually observed in a glass model with the aid of the phosphorescent particle flow-visualization technique (reference 2).

It is known that the secondary flow which exists in a pipe bend or a helix distorts the axial velocity structure in an asymmetrical fashion. Specifically, the fluid velocities are high near the outer wall and low near the inner wall. The secondary flow patterns are generated because of the centrifugal forces that exist in the system. Some typical qualitative velocity distributions in the established flow region for a range of Reynolds numbers were determined for the ANP In-pile Loop helix and are shown plotted in Figure 2. Note, that the degree of distortion decreases as the Reynolds number increases and the flow becomes more turbulent in nature. Also, observe that the profile at Re = 2,700 appears to be a distorted parabola which merely reflects the known fact that the critical Reynolds numbers in helical pipes are significantly higher (about 7,000 to 9,000) than those in straight pipes.

Heat Transfer

Figure 3 presents a schematic diagram of the volume-heat-source helix experiment. A sulfuric acid solution (12% acid by weight) was circulated through

UNCLASSIFIED
ORNL-LR-DWG. 16331

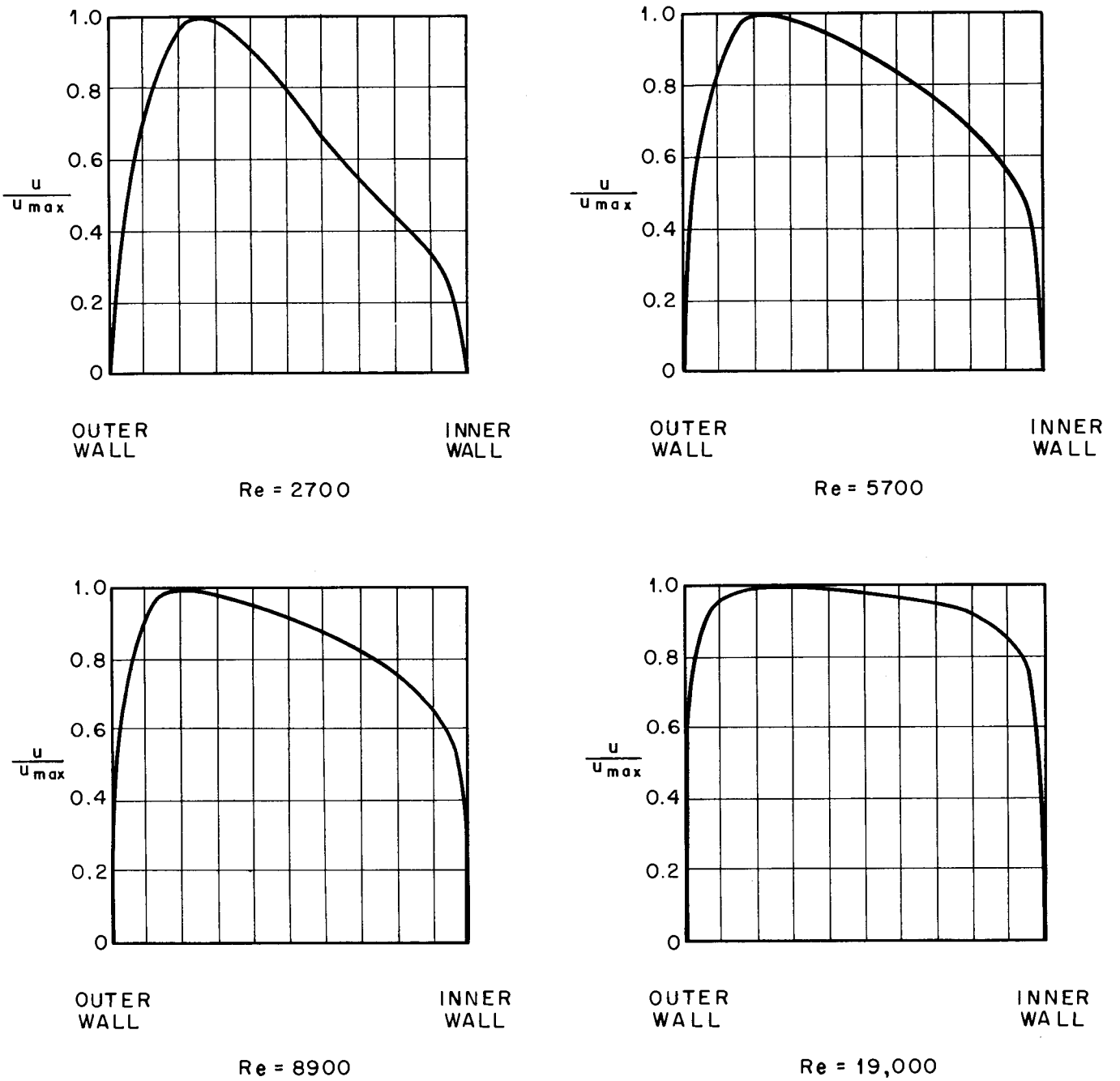

Fig. 2. Typical Qualitative Velocity Profiles for the ANP "In-Pile Loop Helix" at L/D = 99.

UNCLASSIFIED
ORNL-LR-DWG. 16332

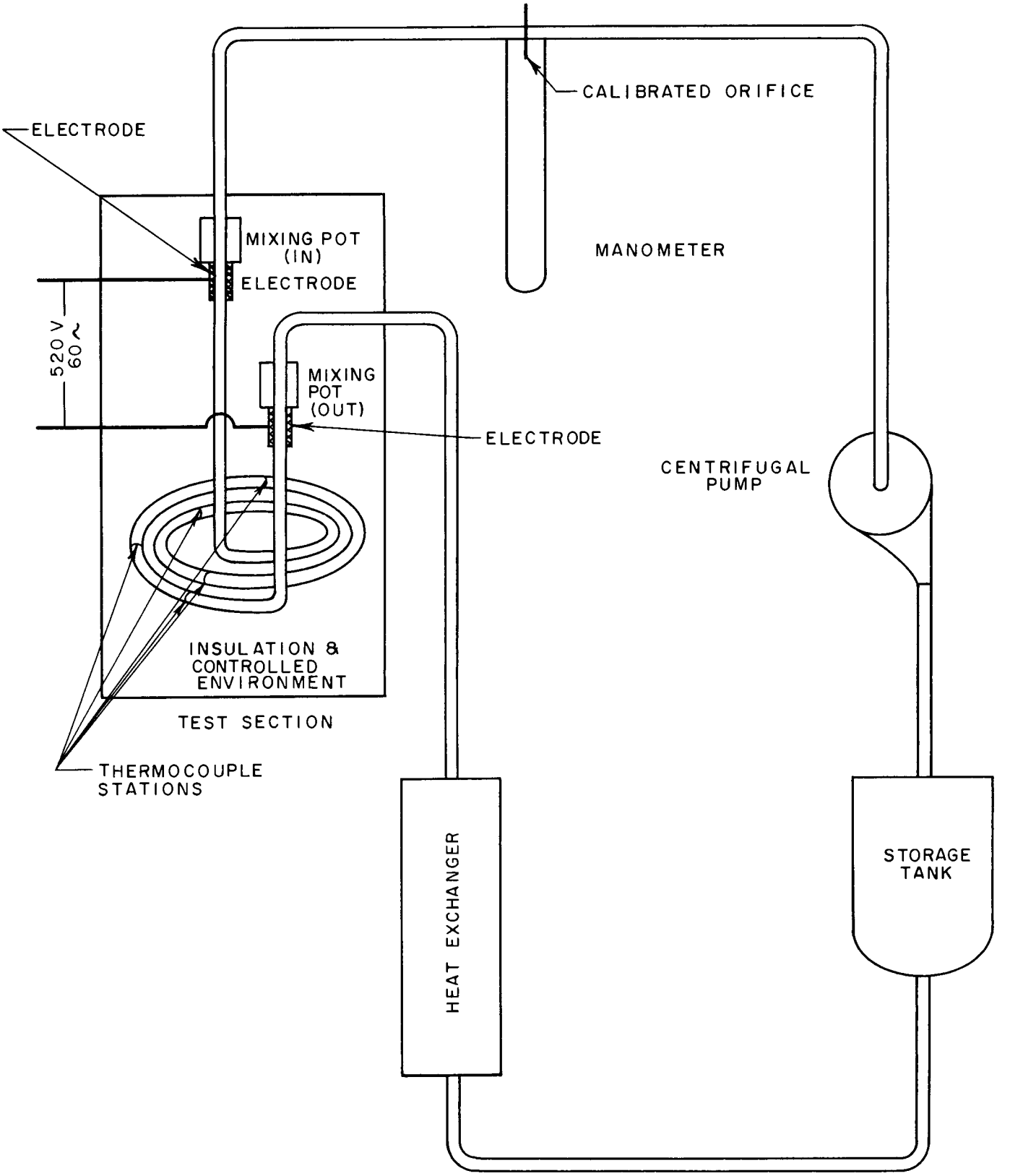

Fig. 3. Diagramatic Sketch of the Volume Heat Source Flow System with ANP "In-Pile Loop Helix" Test Section.

a large scale model of the actual ANP In-pile Loop helix. An electric current was passed through the flowing electrolyte in the helix by means of platinum ring electrodes located at each end of the helix. The outer helix surface was insulated which was very nearly the case in the actual system. The helix was so instrumented with thermocouples that peripheral wall temperatures and mixed-mean fluid temperatures into and out of the system could be measured. Acid solution flow rates were also determined during the experiment. Heat balances were within $\pm$ 7.0 percent of being perfect.

A typical set of axial temperature distributions in the helix system with insulated walls is shown plotted in Figure 4, where the conditions of the experiment are also given. Note that the inner wall temperatures are significantly higher than the outer wall temperatures; the latter fall near the mixed-mean fluid temperatures. The inner helix wall temperatures are higher than the outer wall temperatures because the fluid velocities are lower near the inner wall than those near the outer wall.

In the Reynolds number range of 6,000 to 20,000, the inner-outer helix wall temperature difference varies inversely with the Reynolds number (see Figure 5); one would expect the radial temperature structure to become more uniform as the Reynolds number or the turbulence level increases. A single predicted temperature difference is also shown in Figure 5, the details of which are described in the following section.

Detailed peripheral wall temperature profiles were measured in the helix system at several axial stations. Typical profiles in dimensionless form at L/D = 99 can be seen in Figure 6 for two different flow conditions. The profiles peak sharply at the inner wall.

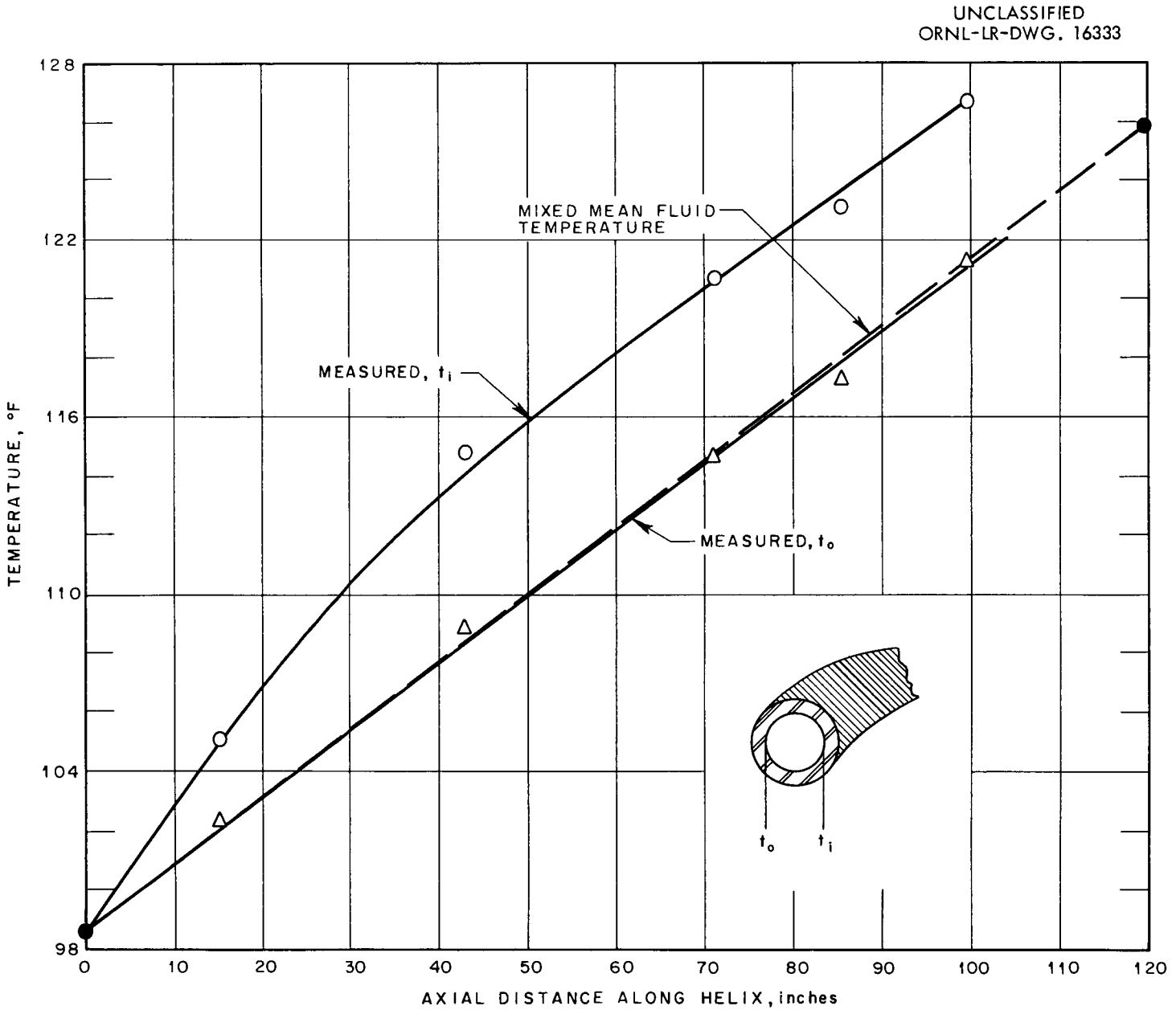

Fig. 4. Temperature Structure in a Helical Pipe with Insulated Walls. Re = 5700; Pr = 5.0; $\overline{W} = \frac{3.65 \times 10^5 \text{ Btu}}{\text{ft}^3 \text{ hr}}$

UNCLASSIFIED
ORNL-LR-DWG. 16334

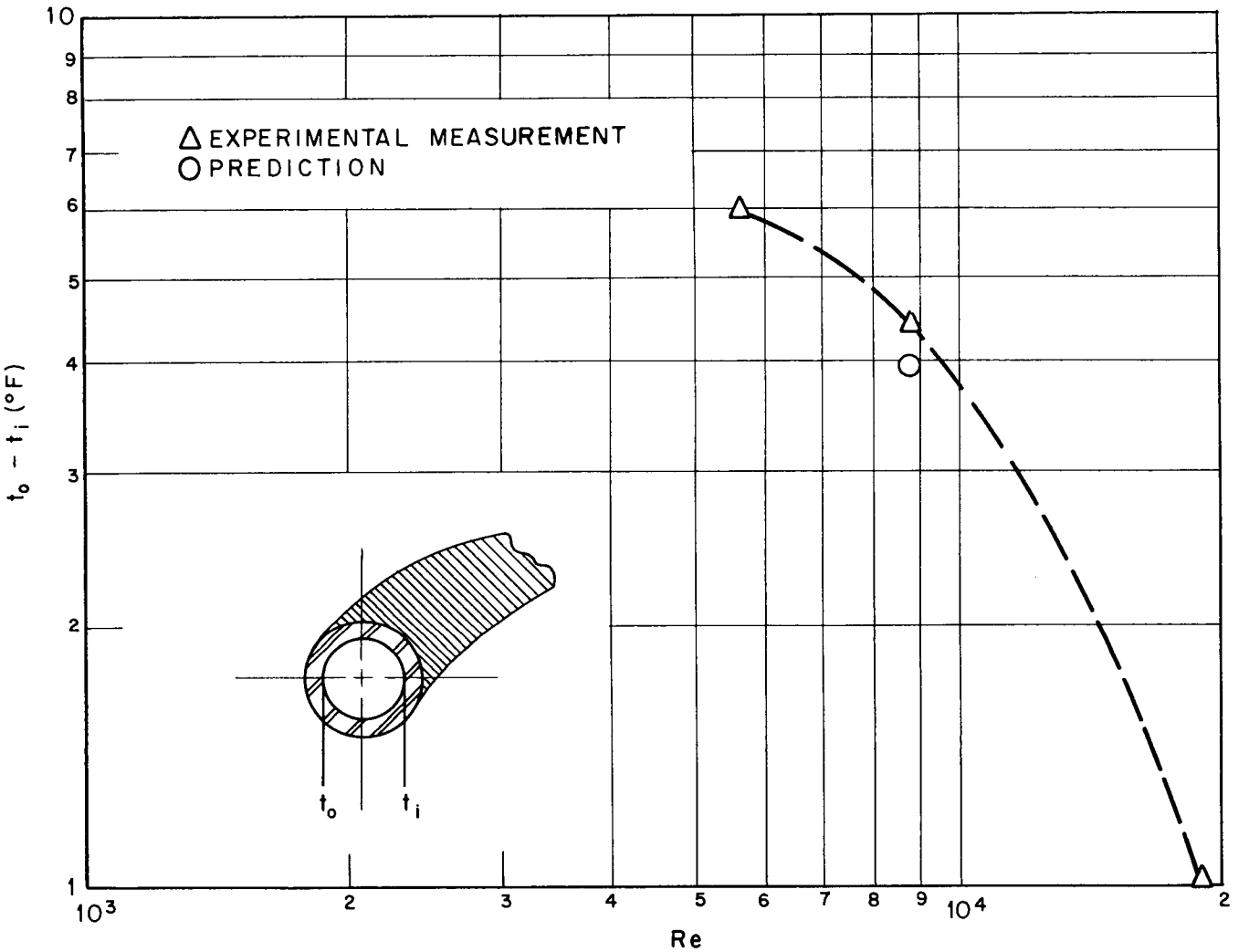

Fig. 5. Inner—Outer Wall Temperature Differences for Established Flow in the ANP In-Pile Helix as a Function of Reynolds Number.

UNCLASSIFIED
ORNL-LR-DWG. 16335

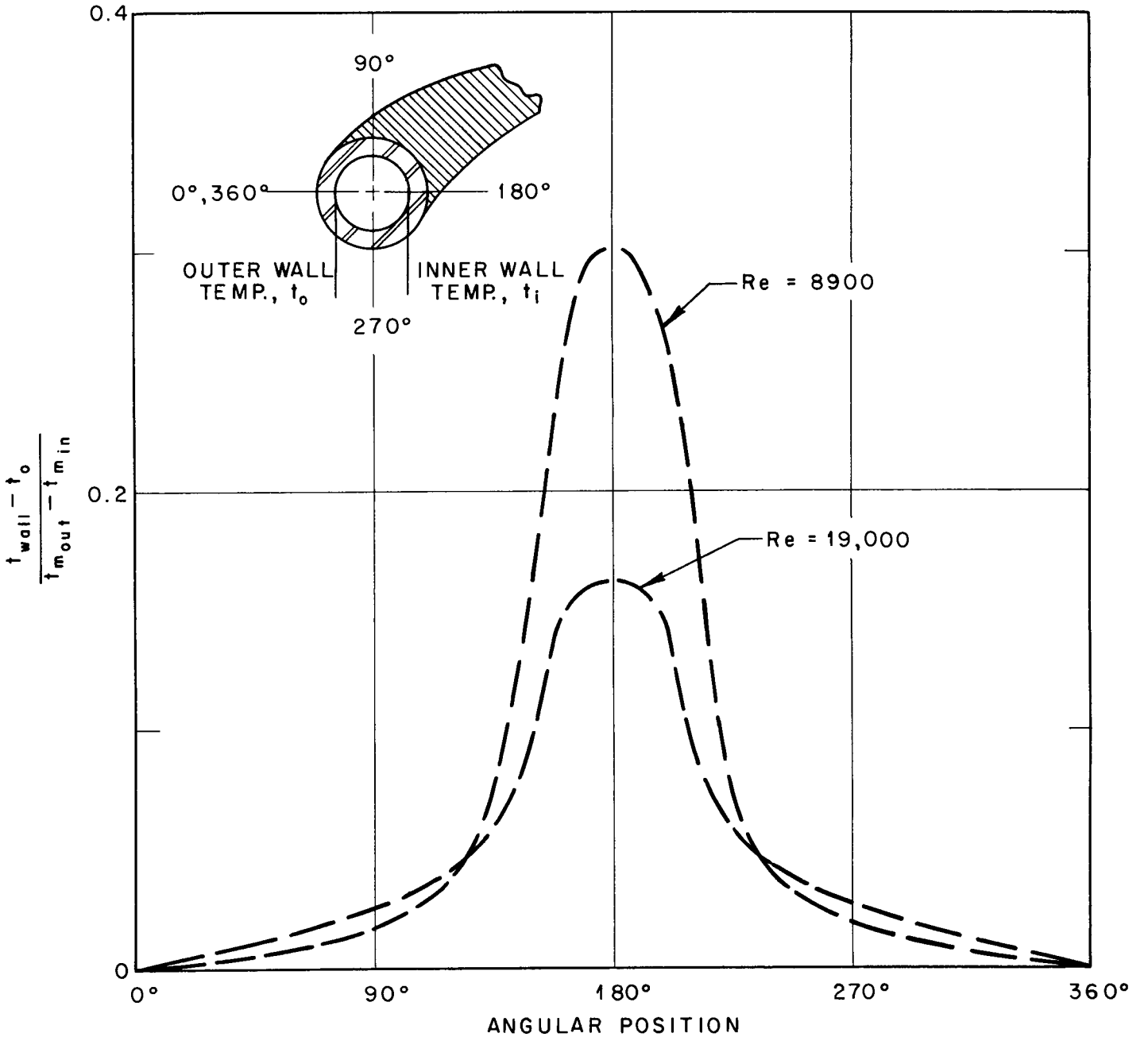

Fig.6. Typical Peripherial Wall Temperature Distributions as a Fraction of the Total Mixed Mean Temperature Rise (L/D = 99)

COMPARISON OF EXPERIMENTAL AND PREDICTED TEMPERATURE DISTRIBUTIONS

An approximate mathematical analysis of the temperature structure within a fuel flowing in a helical pipe is presented in the Appendix, which accounts for the asymmetrical fluid velocity and eddy diffusivity distributions which are present. The results of the prediction are shown in Figure 7, together with the experimental measurements. The calculated inner-outer wall temperature difference was found to be within 12 percent of the experimental value for the specific case which was studied.

UNCLASSIFIED
ORNL-LR-DWG. 16336

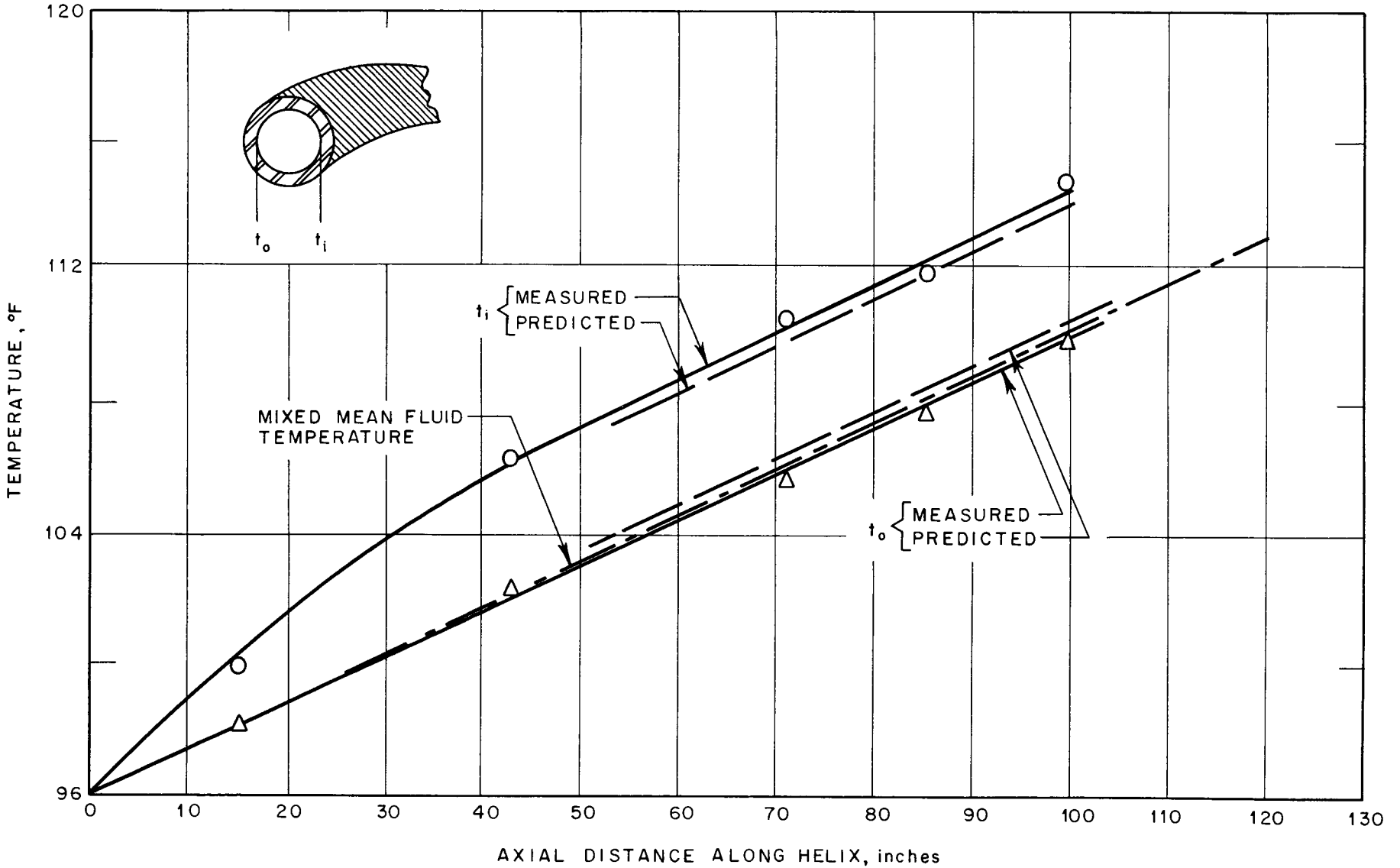

Fig. 7. Temperature Structure in a Helical Pipe with Insulated Walls. Re = 8900; Pr = 5.4; $\overline{W} = \frac{3.65 \times 10^5 \text{ Btu}}{\text{ft}^3 \text{ hr}}$

CONCLUDING REMARKS

Several broad observations about the helix of the ANP In-pile Loop can be made on the basis of the fluid flow and heat transfer research which has been conducted:

1) Asymmetrical velocity distributions exist within the fluid which flows through the helix. The velocities are high near the outer wall and low near the inner wall.
2) Asymmetrical temperature distributions exist in the walls of a helical pipe system as well as within fluids flowing through it, if volume heat sources exist in the fluid or wall. The inner wall temperatures can be significantly higher than the outer wall temperatures.
3) An approximate temperature solution for the case of turbulent flow in a helical pipe containing a fluid with a volume heat source has been outlined; it can be used to estimate the temperature asymmetry in such systems.
4) When the helix radius of curvature is small, the pipe radius is large, and the Reynolds number is low, large differences in inner and outer wall temperatures can exist in a helix system. Under these circumstances, the complicated corrosion and mass transfer processes in an In-pile Loop system of the ANP type may be significantly influenced.

APPENDIX

APPROXIMATE SOLUTION FOR THE RADIAL FLUID TEMPERATURE STRUCTURE IN THE HELIX SYSTEM

In order to derive an exact temperature solution for the helix system under study in this report (as was done for the pipe system in reference 3), it would be necessary to have very detailed information about the complicated hydrodynamic structure which is not available at this time. In addition to the velocity distribution, the shear stress structure would also have to be known in order to determine the eddy diffusivity distribution. In lieu of an exact analysis, the following approximate solution is presented at this time.

In order to determine the difference between the inner and outer wall temperatures of the helix, the differences between the minimum fluid temperature and the inner and outer wall temperatures were first calculated. This step was carried out on the presumption that heat transfer in the "inner and outer sectors" (see Figure 8) is not influenced significantly by heat transfer in adjacent sectors. This postulate is a good one if the controlling thermal resistances are in the flow layers adjacent to the duct walls; this condition exists for the low Reynolds number system being considered. Further, it is postulated that there is no peripheral heat transfer in the pipe wall.

The experimental velocity measurements in a pipe bend by Adler (reference 4) were extrapolated to the curvature condition of the ANP helix; the velocity profile through the inner and outer sectors of the helix is shown in Figure 9 expressed in terms of a ratio of local velocity to maximum velocity. The velocity distribution for the inner flow sector (which is the important one

UNCLASSIFIED
ORNL-LR-DWG. 16337

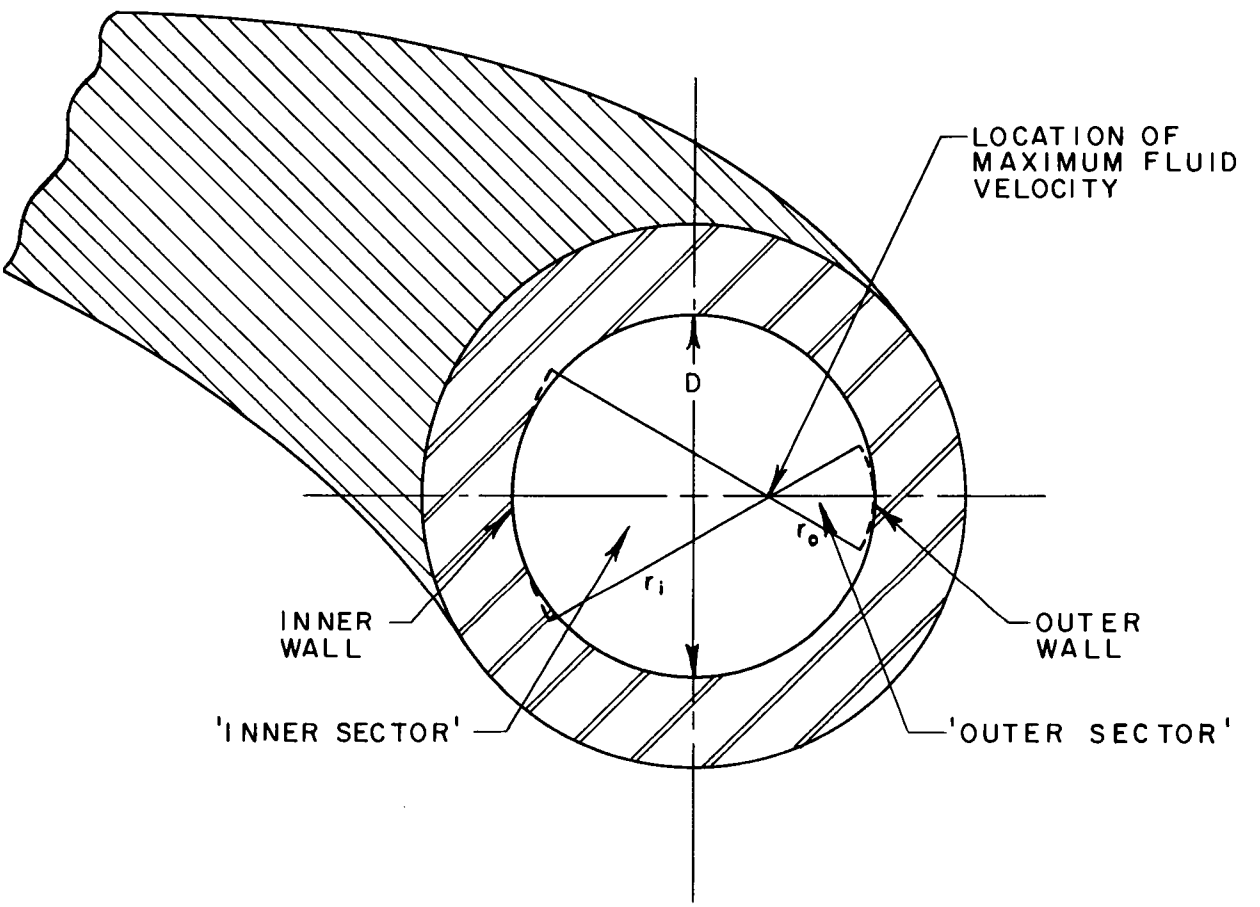

Fig. 8. Inner and Outer Flow Sectors in Helix System.

UNCLASSIFIED
ORNL-LR-DWG. 16338

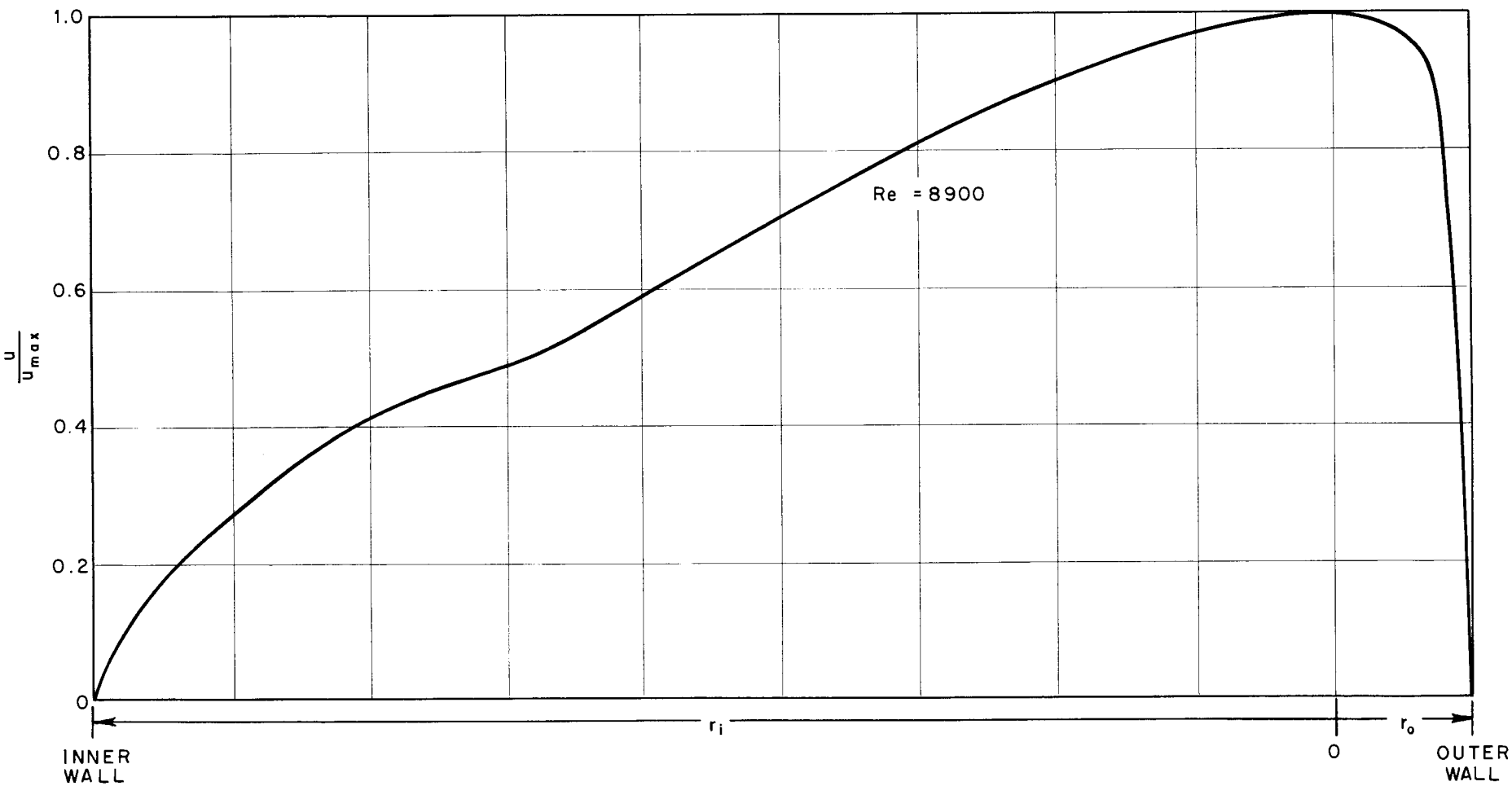

Fig. 9. Velocity Profile in a Helix Having a Pipe to Helix Radius Ratio of 1/12 (Extrapolated from Adler's Measurements)

from a heat transfer standpoint) was found to be representable by a 1/1.6 power law. The outer flow sector (which is of less importance from a heat transfer standpoint) was represented by the usual 1/7 power law. The Reynolds moduli for the inner and outer flow sectors were next evaluated in terms of the pipe Reynolds number. From Figure 9, the sector radii were found to be, $r_i = 0.9D$ and $r_o = 0.1D$. The mean velocity to maximum velocity ratios for the inner and outer sectors were calculated on the basis of the 1/1.6 and 1/7 power law velocity distributions, respectively, and were determined to be $\frac{\bar{u}_i}{u_{max}} = \frac{1}{2.14} = 0.47$, and $\frac{\bar{u}_o}{u_{max}} = \frac{1}{1.23} = 0.82$. On the basis of flow continuity, the mean velocity over the whole flow cross section to the maximum velocity (Figure9) was estimated to be about, $\frac{\bar{u}}{u_{max}} = 0.57$. Thus, the sector to pipe mean velocity ratios were found to be, $\frac{\bar{u}_i}{\bar{u}} = \frac{0.47}{0.57}$ and $\frac{\bar{u}_o}{\bar{u}} = \frac{0.82}{0.57}$. Hence, the desired Reynolds moduli for the inner and outer flow sectors are

$$Re_i = \frac{\bar{u}_i 2r_i}{\nu} = \frac{0.47\ \bar{u}}{0.57}\ \frac{1.8D}{\nu} = 1.5\ Re = 1.5\ (8{,}900) = 13{,}300$$

and

$$Re_o = \frac{\bar{u}_o 2r_o}{\nu} = \frac{0.82\ \bar{u}}{0.57}\ \frac{0.2D}{\nu} = 0.29\ Re = 0.29\ (8{,}900) = 2{,}580.$$

The volumetric heat source, W, was not quite uniform across the flow cross sectional area in the glass helix system because the electric potential gradient was not quite constant with radius from the helix center. The volume heat source in a differential volume is,

$$W = 3.413\ \frac{dP}{dV} \tag{1}$$

where P is the electrical heat source and V is the volume. The electrical heat source can be expressed as

$$dP = \frac{(dE)^2}{R_e} = \frac{(dE)^2}{\rho_e r_h \frac{d\Phi}{dA_e}} \tag{2}$$

The differential volume can be written in the form

$$dV = r_h d\Phi dA_e \tag{3}$$

Upon substituting equations (2) and (3) into equation (1) and simplifying, one obtains,

$$W = \frac{1}{\rho_e}\left(\frac{dE}{r_h d\Phi}\right)^2 \tag{4}$$

The angular voltage gradient in a helix is a constant and thus

$$W = \frac{\text{constant}}{r_h^2} \tag{5}$$

From equation (5) it was determined that the volume heat source in the fluid at the inner wall was only 30 percent greater than the value at the apex of the inner sector. Also, the volume heat source in the fluid at the outer wall was only 7 percent smaller than the value at the apex of the outer sector. Consequently, a uniform volume-heat-source distribution across the helix flow cross-section equal to the mean value was used in the following analysis.

The boundary value problem being considered for each sector under established flow conditions is defined as follows:

$$\left.\begin{aligned} &\frac{u(r)\overline{W}r}{\overline{u}_s c_p \gamma} - \frac{\overline{W}r}{c_p \gamma} = \frac{d}{dr}\left[(a + \epsilon)r\frac{dt}{dr}\right] \\ &\frac{dq}{dA}(r = r_o, r_i) = 0 \\ &t\,(r = r_d) = t_d \end{aligned}\right\} \tag{6}$$

The radial heat flow in the helix system can be obtained by integrating the differential equation of equations (6). The velocity distribution in the outer flow sector possessed a 1/7 power-like velocity profile, therefore, the radial heat flow solutions previously developed for the pipe system (reference 3) can

be used. The radial heat flow distribution in the inner flow sector was obtained by integrating the above differential equation utilizing a 1/1.6 power law velocity relation[1],

$$\frac{\frac{dq}{dA}}{\frac{\overline{W}r_i}{2}} = \frac{2}{1-n}\int_0^n \left(\frac{u}{\bar{u}_i}\right)(1-n)dn + \left[\frac{-2n + n^2}{1-n}\right]$$

$$= \frac{4.28}{1-n}\left[0.615\ n^{1.625} - 0.381\ n^{2.625}\right] + \left[\frac{-2n + n^2}{1-n}\right] \qquad (7)$$

Equation (7) was evaluated and is shown graphed in Figure 10 together with the corresponding heat flow distribution in a pipe at a Reynolds number of 13,000 for purposes of comparison. The radial heat flow distribution for the 1/1.6 power law is about 1.8 times greater[2] than the corresponding quantity for a pipe velocity distribution.

The differences between inner and outer wall temperatures were calculated for the helix system for the specific conditions, Re = 8,900, Pr = 5.4, $\overline{W} = 3.65 \times 10^5$ Btu/hr ft^3, D = 1/12 ft, and k = 0.33 Btu/hr ft^2 (^{o}F/ft).

Inner Sector Calculation

It is presumed that the eddy diffusivity structure in the sector is uniquely defined by the Reynolds number and geometry of the system. Consequently the results of the previous pipe analysis (references 3 and 5) can be used if they are modified to account for the fact that the radial heat flow for the 1/1.6 power law sector system is on the average 1.8 times greater than that for a pipe

---

1. The velocity function of the inner flow sector is represented by the expression, $u = 2.14\ \bar{u}_i n^{1/1.6}$

2. This is a mean value which is weighted to account for the important thermal resistances in the vicinity of the sector wall.

UNCLASSIFIED
ORNL-LR-DWG. 16339

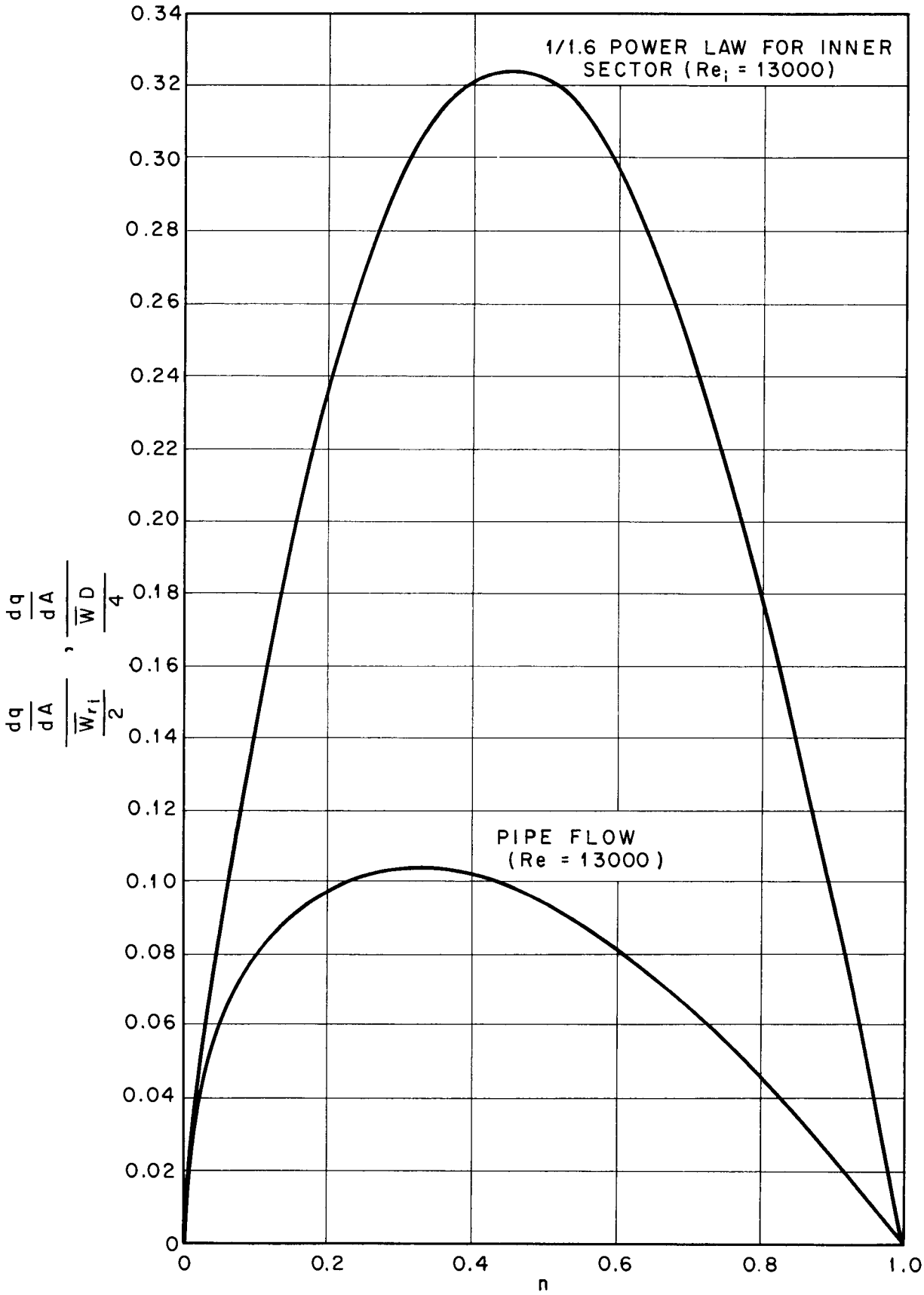

Fig. 10. Comparison of Dimensionless Radial Heat Flow Distributions for Inner Sector and Pipe (Insulted Walls)

type of velocity structure. From Table 1 in reference 5, the dimensionless difference between the wall and fluid centerline[3] temperatures for the inner sector conditions was found to be 3.8×10^{-4}. Thus,

$$\frac{t_i - t_{\mathbb{C}}}{\frac{\bar{W}r_i^2}{k}} = 3.8 \times 10^{-4} \; \frac{\left(\frac{\frac{dq}{dA}}{\frac{\bar{W}r_i}{2}}\right)_{1/1.6 \text{ vel. distr.}}}{\left(\frac{\frac{dq}{dA}}{\frac{\bar{W}D}{4}}\right)_{\text{pipe vel. distr.}}}$$

or $$t_i - t_{\mathbb{C}} = (3.8 \times 10^{-4}) \frac{(3.65 \times 10^{+5})\ (562 \times 10^{-5})}{(0.33)} \ (1.8) = 4.25^{\circ}\ \text{F}$$

Outer Sector Calculation

From Table 1 in reference 5, the dimensionless difference between the wall and fluid centerline temperatures for the outer sector conditions was found to be about 4.8×10^{-3}. Thus,

$$\frac{t_o - t_{\mathbb{C}}}{\frac{\bar{W}r_o^2}{k}} = 4.8 \times 10^{-3}$$

or $$t_o - t_{\mathbb{C}} = (4.8 \times 10^{-3}) \frac{(3.65 \times 10^{5})\ (69.3 \times 10^{-6})}{(0.33)} = 0.37^{\circ}\ \text{F}$$

Thus the difference between the inner and outer wall temperatures in the established flow region of the helix for the specific conditions given above is,

$$t_i - t_o = 4.25 - 0.37 = 3.9^{\circ}\ \text{F}$$

This predicted temperature difference is within 12 percent of the experimental temperature difference which was 4.4° F. The comparision appears in Figure 7.

---

3. Fluid centerline refers to the apex of the flow sector.

REFERENCES

1. Palmer, L. D., Winn, G. M., Poppendiek, H. F., "Investigation of Fluid Flow in Helical Bends of the ANP In-pile Loop", ORNL CF 55-6-183

2. Palmer, L. D., Winn, G. M., "A Feasibility Study of Flow Visualization Using a Phosphorescent Particle Method", ORNL CF 54-4-205

3. Poppendiek, H. F., Forced-Convection Heat Transfer in Pipes with Volume Heat Sources within the Fluids, Chem. Engr. Progress Symposium Series, Vol. 50, No. 11 (1954)

4. Adler, M., Stromung in gekrummten Rohren, Zeitschrift fur Angewandte Mathematik and Mechanik 14, No. 5: 257-276 (1934)

5. Poppendiek, H. F., Palmer, L. D., "Application of Temperature Solutions for Forced Convection Systems with Volume Heat Sources to General Convection Problems", ORNL 1933, Sept. 1955